

Structure of domain walls in the surface layer of iron single crystals

V. E. Zubov, G. S. Krinchik, and A. D. Kudakov

M. V. Lomonosov State University, Moscow

(Submitted 14 April 1988)

Zh. Eksp. Teor. Fiz. **94**, 243–250 (December 1988)

A magneto-optic method was used to study the fine structure of 180° domain walls on the surface of iron single crystals. The Néel and normal (to the surface) components of the magnetization changed sign along a section perpendicular to a wall. Characteristics of the fine structure of a wall were linked uniquely to the direction of asymmetric bending in the surface layer. The distributions of three components of the magnetization were determined in one section across a domain wall. Two types of structure singularities were observed for a domain wall, associated with the emergence of vertical Bloch lines on the surface; singularities of the Bloch point type were also observed. A sideways displacement of a wall by a distance of $\approx 0.4 \mu\text{m}$ was observed during motion along a domain wall in the case of two of these special singularities of the wall. The structure of a 90° domain wall was investigated for the first time. This wall was also asymmetric in the surface layer; its effective thickness on the surface was three times the thickness in the bulk.

1. INTRODUCTION

The main types of one-dimensional walls in ferromagnets were considered by Landau and Lifshitz¹ and by Néel.² Investigations of the structure of domain walls in thin films and near the surfaces of bulk crystals led Hubert³ and LaBonte⁴ to propose a two-dimensional model of the distribution of spins in a domain wall characterized by the presence of a Néel (perpendicular to the plane of a domain wall) component of the magnetization. This model is known as an asymmetric Bloch wall.³ On approach to the surface in a bulk crystal a wall broadens by a factor of 3–4 (Ref. 5). Experimental electron-microscopic investigations of the structure of a 180° domain wall in iron films⁶ showed that a wall had an asymmetric structure, in agreement with the theoretical predictions. A magneto-optic investigation of 180° domain walls in bulk iron single crystals revealed that the wall became several times thicker on approach to the surface and had a Néel component close to the maximum possible.⁷ The thickness of a 180° domain wall in the bulk of an iron crystal was calculated by Lilley⁸ who obtained the value $0.23 \mu\text{m}$. Measurements reported by Suzuki and Suzuki,⁹ made using an electron microscope, showed that an increase in the thickness of iron films increased the thickness of the domain walls, which reached a maximum value that agreed with Lilley's estimate. Green and Leaver¹⁰ as well as Proto and Lawless¹¹ used the same method to observe asymmetric 90° domain walls in nickel and iron films.

The use of an electron microscope makes it possible to study the structure of domain walls in ferromagnetic films. However, the information on the wall structure is then averaged over the film thickness. Magneto-optic effects observed in reflected light provide a satisfactory means for the study of surface magnetic structures in ferromagnets.

We used an improved magneto-optic setup with micron resolution to continue the study of the structure of domain walls in iron single crystals, which was begun earlier.⁷ We studied the fine structure of 180° domain walls and established a relationship between the fine structure and the direction of asymmetric bending of a wall near the surface. We considered characteristic features of the structure of a domain wall associated with emergence of vertical Bloch lines

on the surface and a singularity of the Bloch point type in domain walls. We also studied the structure of 90° domain walls.

2. MEASUREMENT METHOD AND SAMPLES

Our experimental investigation was carried out using a magneto-optic micromagnetometer built around an MIM-8 metallographic reflecting microscope. This micromagnetometer operates by measuring in the image plane of the microscope, changes in the intensity of light reflected from a microregion of a ferromagnet when its magnetization is reversed. The operations required to measure any particular magneto-optic effect were described in detail in Ref. 7. Improvements in the apparatus compared with that described in Ref. 7 included the use of a more powerful DKSSh-150 xenon lamp, automation of the measurement process, and widening of the frequency range. Consequently, the sensitivity of our measurements of the relative change in the intensity of light was increased by an order of magnitude and amounted to $\sim 10^{-5}$ in studies of a part of a surface of a ferromagnet of $\sim 1 \mu\text{m}^2$ area at frequencies from 20 Hz to 100 kHz. The magnetization components lying in the magnetic mirror plane were determined using the linear (in the magnetization) equatorial and meridional Kerr effects, as well as the quadratic (in the magnetization) orientational magneto-optic effect.⁷ The component perpendicular to the surface of a sample was found using the polar Kerr effect.

We used single-crystal iron whiskers prepared by the method of chemical reduction of iron halides in hydrogen. Our samples were rods of square cross section and $\approx 0.05 \times 0.05 \text{ mm}$ dimensions; their length was $\approx 10 \text{ mm}$ and they had natural optically "perfect" faces of the (001) type. The edges of the whiskers coincided with directions of the [001] type. Our samples contained 180° domain walls located at the center of a sample along the whisker axis and parallel to the side faces. A 180° domain wall could be interrupted by 90° walls bounding prismatic domains with the magnetization perpendicular to the axis of the sample. The number of the latter domains ranged from 0 to 5. The domain structure was visualized under a microscope using a ferromagnetic liquid.

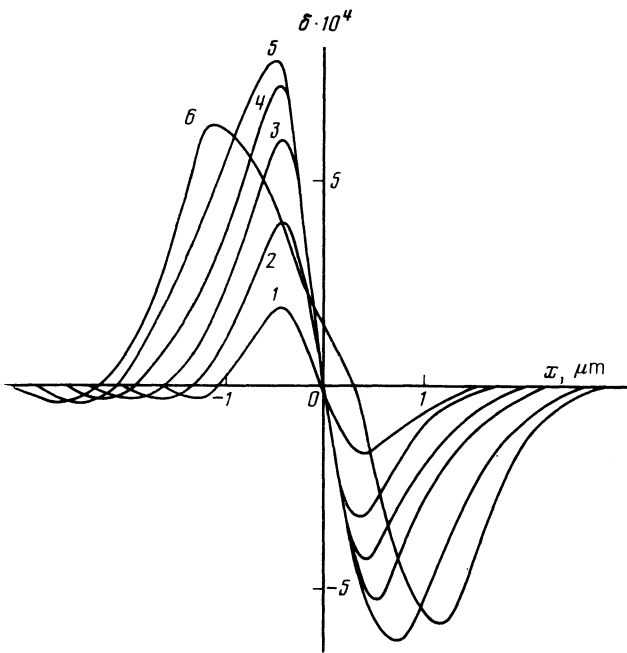


FIG. 1. Curves representing the equatorial Kerr effect due to the component I_x in a domain wall, plotted for different values of Δ (μm): 1) 0.1; 2) 0.2; 3) 0.3; 4) 0.4; 5) 0.5; 6) 0.9.

3. INVESTIGATION OF 180° DOMAIN WALLS

Figure 1 shows a family of the equatorial Kerr curves representing the Néel component of the magnetization of the domain wall I_x on the surface of a crystal. Different curves were obtained for different amplitudes Δ of vibrations of a domain wall induced by an oscillatory magnetic field directed along the whisker axis. The equatorial Kerr effect appeared because of a change in I_x due to domain wall vibrations. The x and y coordinate axes were in the plane of the wall; the y axis was parallel to the long axis of the sample and the z axis was perpendicular to the face. The value of Δ depended linearly on the amplitude of the applied magnetic field H_0 , which was established (as in Ref. 7) from the way the distance d between two large extrema of the equatorial Kerr curve due to the component I_x depended on the value of H_0 . The amplitude Δ could also be determined with the aid of the domain effect,⁷ i.e., using the equatorial Kerr effect due to the component I_y . In strong fields H_0 the region where the equatorial Kerr effect differed from zero was then governed by the value of Δ . In weak fields H_0 we could determine Δ by approximating the results with a linear dependence $\Delta(H_0)$ in the limit $H_0 \rightarrow 0$. The results of measuring Δ by these two methods agreed satisfactorily. The curves in Fig. 1 were asymmetric and the behavior of the maxima and minima of the alternating curves changed as Δ increased. A small minimum was observed to the left of the main extrema. The nature of the asymmetry of the main extrema and the position of the small minimum were related uniquely, as demonstrated below, to the direction in which the domain walls bent at the surface. The domain wall asymmetry was manifested also by changes in the polar Kerr curves due to a change in the orientation of the magnetization in a domain wall for different values of Δ .

Figure 2 shows the dependence of the equatorial, meridional, and polar Kerr effects on x obtained in one section of

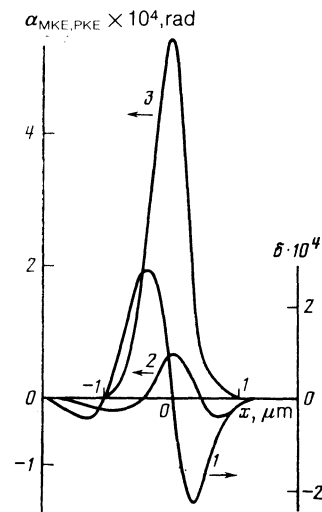


FIG. 2. Curves representing (1) the equatorial Kerr effect, (2) the meridional Kerr effect, and (3) the polar Kerr effect (PKE) due to the components I_x , I_y , and I_z in a domain wall. All the curves were determined for the same section across a domain wall and the same value of $\Delta = 0.1 \mu\text{m}$.

a domain wall for the same values of $\Delta = 0.1 \mu\text{m}$ and due to the components I_x , I_y , and I_z obtained in a domain wall. Clearly, the polar Kerr effect changed its sign twice along a section across a wall. Moreover, the right- and left-hand parts of the polar effect were asymmetric relative to the central maximum. It was found earlier⁷ that the polar Kerr effect exhibited only one sign reversal: the inadequate sensitivity of the older apparatus failed to reveal the fine structure of the distribution of the component I_z in a domain wall. The nature of the curves representing the polar Kerr effect indicated an asymmetric distribution of I_z in the wall, in agreement with the results of an investigation of the component I_x .

In low fields H_0 , when $\Delta \ll d_0$ ($d_0 \approx 0.7 \mu\text{m}$ is the effective thickness of a domain wall; this thickness d_0 was defined in Ref. 7 as the limit which d approached when $\Delta \rightarrow 0$), the curves in Fig. 1 were proportional to $\partial I_x / \partial x$. The condition $\Delta \ll d_0$ was satisfied also as the curves shown in Fig. 2 changed.

Numerical integration could be used to reconstruct the dependence of I_x , I_y , and I_z on x from the curves representing the equatorial, meridional, and polar Kerr effects. The

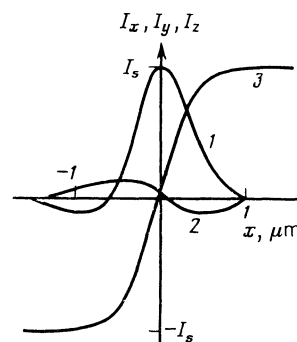


FIG. 3. Dependences of the three components of the magnetization in a 180° domain wall, reconstructed from the magneto-optic effects presented in Fig. 2 for 1) I_x ; 2) I_y ; 3) I_z .

results of such integration are presented in Fig. 3, demonstrating clearly the asymmetry of the distributions of the components I_x and I_z of a wall. The normalization coefficient necessary for plotting the $I_x(x)$ curve was found by measuring the equatorial Kerr effect δ_0 under saturation conditions, due to the component I_y , i.e., when magnetization reversal changed I_y from $-I_s$ to $+I_s$. The normal value of the meridional Kerr effect under saturation conditions was determined at high values of Δ and in the case of the polar Kerr effect this was deduced from Ref. 12.

In the case of large values of Δ the equatorial Kerr effect was governed, in particular, no longer just by $\partial I_x / \partial x$ but also by higher derivatives:

$$\frac{\delta}{\delta_0} \approx \Delta \frac{\partial}{\partial x} \left(\frac{I_x}{I_s} \right) + \frac{\Delta^3}{8} \frac{\partial^3}{\partial x^3} \left(\frac{I_x}{I_s} \right). \quad (1)$$

Analysis indicated that the contribution of the second derivative $\partial^2 I_x / \partial x^2$ was zero. The results of calculations of the equatorial Kerr effect carried out using the above expression and the dependence $I_x(x)$ of Fig. 3 are presented in Fig. 4. The behavior of the principal extrema in Fig. 4 on increase in Δ agrees with their dependence observed experimentally (Fig. 1).

One may ask whether the small minimum exhibited by the equatorial Kerr effect (Fig. 1) is not due to the fine structure of domain walls on the surface, but is a consequence of the diffraction of light by the domain walls. It was shown in Ref. 13 that reversal of the sign of the magneto-optic effect observed in a very narrow linear magnetic object (on the assumption that the width of the object is much less than the wavelength of light λ) in the image plane of an optical instrument occurs at a distance corresponding to $0.5\lambda \approx 0.3 \mu\text{m}$ in the object plane and the distance from a small minimum in Fig. 1 to the neighboring maximum of the equatorial Kerr effect is $0.7-0.8 \mu\text{m}$. It therefore follows that this small minimum does indeed reflect singularities of the structure of a domain wall. The diffraction in the wall affects measurements of the magneto-optic effects by flattening the observed

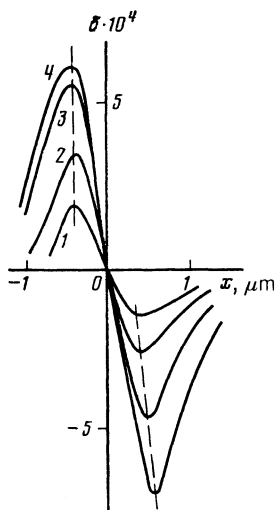


FIG. 4. Curves representing calculations of the equatorial Kerr effect due to I_x plotted for different values of Δ (μm): 1) 0.1; 2) 0.2; 3) 0.3; 4) 0.5. The calculations were made using Eq. (1) and the $I_x(x)$ curve from Fig. 3.

singularities in the dependence of these effects on the spatial coordinates.

An investigation of domain walls in the region where the direction of bending reverses its sign makes it possible to relate the bending at an arbitrary point of a wall to the observed asymmetry of the magneto-optic signal from this wall. A structural entity of the Bloch type represented in the domain wall observed when the direction of bending of the wall was reversed and a strong sideways displacement of the wall by $0.4 \mu\text{m}$ took place, was described recently in Ref. 14. The observed shift of the wall made it possible to determine the direction of bending of the wall on the surface. The smallest of the three extrema of the equatorial Kerr effect (Fig. 1) was always located on the side opposite to the direction of bending of the domain wall. Therefore, the profile of the alternating curve representing the equatorial Kerr effect in a wall could be used to determine reliably the direction of bending of the wall at the surface.

In addition to a Bloch point, we could postulate the existence of two further singularities of the structure of an asymmetric domain wall associated with the emergence of vertical Bloch lines on the surface. These singularities were observed experimentally and described in Ref. 14. For one of the singularities the direction of bending of the domain wall was the same on opposite sides of a vertical Bloch line, whereas for the other it was different. Since in the bulk of a crystal the signs of I_z in a domain wall should differ for different sides of a vertical Bloch line, it follows that in the former case the signs of I_x on the opposite sides of a vertical Bloch line on the surface should be different, whereas in the latter case they should be the same. Moreover, moving along a domain wall across a vertical Bloch line should not give rise to sideways displacement of a domain wall on the surface in the former case, whereas in the latter case such a displacement should be $\approx 0.4 \mu\text{m}$, exactly as in the case of a Bloch point.

The results of our investigation of domain walls on the surfaces of iron crystals agree basically with a model of an asymmetric Bloch 180° wall described by Hubert^{3,5,15} and shown in Fig. 5. It is clear from this figure that the following domain wall features appeared in the surface layer. The wall was bent asymmetrically. The value of the Néel component I_x was close to the maximum possible. The thickness of a domain wall on the surface was several times greater than

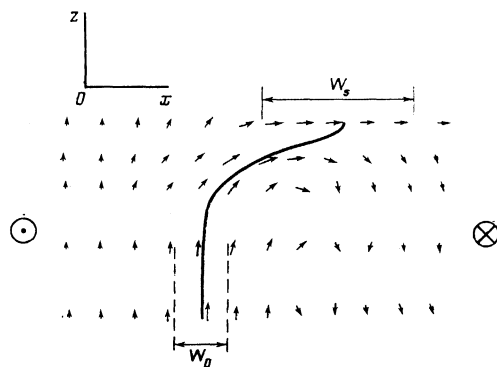


FIG. 5. Model of an asymmetric 180° Bloch domain wall proposed by Hubert³; here, W_0 is the effective thickness of a domain wall in the bulk and W_s is the corresponding thickness on the surface.

the thickness in the bulk. Moreover, the wall on the surface was shifted relative to its position in the bulk by an amount of the order of its half-width on the surface. The component I_z exhibited reversal of the sign in the surface layer. These features of the structure of a domain wall were observed experimentally in the present study. A new result, not predicted by the Hubert model, was observation of an alternating (variable sign) dependence of the Néel component $I_x(x)$ in a domain wall.

The displacement of a domain wall associated with a change of the direction of its bending was quite large, and this displacement was also observed with the aid of a ferromagnetic liquid. The sideways displacements of domain walls in iron whiskers had been observed earlier (using a ferromagnetic liquid) by Hartmann and Mende,¹⁶ but these displacements were attributed by the authors to a tilt of radical Bloch lines as they emerged on the surface. As pointed out above, in the case of 180° domain walls on the surface we could observe structural singularities of three types. Two of these singularities were associated with a displacement of a wall by a distance of $\approx 0.4 \mu\text{m}$: these were a Bloch point and the second case of emergence of vertical Bloch lines on the surface; the third type of singularity did not involve displacement and it represented the first case of the emergence of vertical Bloch lines. In the samples investigated by Hartmann and Mende the situation was clearly such that the emergence of vertical Bloch lines on the surfaces of whiskers occurred only by the second method, i.e., by displacement of a domain wall. This conclusion was drawn on the basis of the observation that successive displacement of a domain wall occurred along a series of vertical Bloch lines and these lines crossed the whole whisker and were observed on the opposite faces. However, we could not say why the emergence of vertical Bloch lines on the surface by the second method was preferred. A possible answer to this question was that vertical Bloch lines emerging on the surface by the first means were simply unobserved because of the absence of sideways displacement of Bloch walls.

4. INVESTIGATION OF 90° DOMAIN WALLS

Figure 6 shows the orientational magneto-optic effect observed for a 90° domain wall and plotted as a function of the coordinate x' perpendicular to the wall (the x' axis was rotated by 45° in the plane of a whisker face relative to the x axis). The distance of the extrema from the point where the effect reversed its sign at low Δ changed differently on increase in Δ . Hence, we concluded that the law describing the x -dependence of the magnetization component perpendicu-

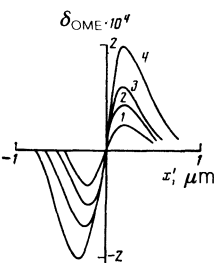


FIG. 6. Orientational magneto-optic effect for a 90° domain wall and different values of Δ (μm): 1) 0.1; 2) 0.12; 3) 0.15; 4) 0.2.

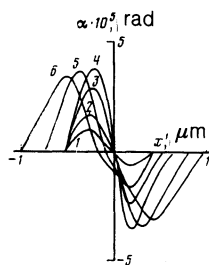


FIG. 7. Polar Kerr effect (α) due to the component I_z in a 90° domain wall, plotted for different values of Δ (μm): 1) 0.07; 2) 0.1; 3) 0.15; 4) 0.2; 5) 0.3; 6) 0.4.

lar to a domain wall differed on the two sides from the center of the wall. This result was similar to that observed for 180° domain walls (Fig. 1), i.e., the structure of 90° domain walls in the surface layer was asymmetric.

Figure 7 shows the x' -dependences of the polar Kerr effect due to the component I_z in a 90° domain wall, obtained for different values of Δ . At low values of Δ ($\approx 0.1 \mu\text{m}$) the distance between the extrema was approximately the same for the orientational magneto-optic effect and the polar Kerr effect, amounting to $\approx 0.4 \mu\text{m}$, which was well above the theoretical value of the effective thickness of a 90° domain wall in the bulk ($\approx 0.08 \mu\text{m}$ was reported in Ref. 8). The diffraction of light could result in broadening of the magneto-optic image of a domain wall by an amount up to $0.2 \mu\text{m}$ (representing $0.1 \mu\text{m}$ on each side).¹³ We could therefore say that the effective thickness of a 90° domain wall on the surface exceeded $0.2 \mu\text{m}$, i.e., it was over 2.5 times greater than the wall thickness in the bulk. Numerical integration of the polar Kerr effect $\Delta = 0.07 \mu\text{m}$ in Fig. 7 yielded a bell-shaped $I_z(x')$ curve. The maximum value of I_z was $0.07 I_s$. The component I_z in a 90° domain wall differed from that in a 180° wall because there was no change of sign along a section across the wall. The observed asymmetry of the distribution of the magnetization in a wall agreed with the model of an asymmetric 90° domain wall described by Hubert.^{3,15}

The curves representing the magneto-optic effects were not affected by an increase in the magnetic field frequency from 20 Hz to 100 kHz; this was true of both 90° and 180° domain walls.

5. CONCLUSIONS

A highly sensitive magneto-optic micromagnetometer was used to find the distribution of three components of the magnetization in 180° domain walls on the surfaces of iron single crystals along a section perpendicular to the wall. Our investigation showed that the structure of domain walls on the surface was complex. The distribution of the Néel component was asymmetric: along the x axis there were regions where I_x had different signs. The $I_z(x)$ dependence also exhibited reversal of the sign. It was shown that the nature of the asymmetry of the distribution of the component I_x was linked uniquely to the direction of bending of the domain wall at the surface. Structural singularities of a domain wall associated with two cases of emergence of vertical Bloch lines on the surface were observed, as well as singularities of the Bloch point type, which were due to asymmetric bending of 180° domain walls.

The magneto-optic methods were used for the first time to investigate 90° domain walls in iron single crystals. An asymmetry of the distribution of the horizontal component of the magnetization was observed along a section perpendicular to a domain wall. The effective thickness of a domain wall on the surface was also determined and it was found to be approximately three times greater than the wall thickness in the bulk.

The observed distribution of the magnetization in a domain wall in the surface layer in iron single crystals agreed basically with the models of asymmetric Bloch 180° and 90° domain walls proposed by Hubert.

The authors are deeply grateful to Yu. P. Gaïdukov and N. P. Danilova for supplying iron single crystals.

¹L. D. Landau and E. M. Lifshitz, *Phys. Z. Sowjetunion* **B 8**, 153 (1935).
²L. Néel, *C. R. Acad. Sci.* **241**, 533 (1955).

³A. Hubert, *Phys. Status Solidi* **32**, 519 (1969).
⁴A. E. LaBonte, *J. Appl. Phys.* **40**, 2450 (1969).
⁵A. Hubert, *Z. Angew. Phys.* **B 32**, 58 (1971).
⁶S. Tsukahara and H. Kawakatsu, *J. Phys. Soc. Jpn.* **32**, 1493 (1972).
⁷G. S. Krinchik and O. M. Benidze, *Zh. Eksp. Teor. Fiz.* **67**, 2180 (1974) [*Sov. Phys. JETP* **40**, 1081 (1975)].
⁸B. A. Lilley, *Philos. Mag.* **41**, 792 (1950).
⁹T. Suzuki and K. Suzuki, *IEEE Trans. Magn.* **MAG-13**, 1505 (1977).
¹⁰A. Green and K. D. Leaver, *Phys. Status Solidi A* **27**, 69 (1975).
¹¹G. R. Proto and K. R. Lawless, *J. Appl. Phys.* **46**, 416 (1975).
¹²G. S. Krinchik and V. A. Artem'ev, *Zh. Eksp. Teor. Fiz.* **53**, 1901 (1967) [*Sov. Phys. JETP* **26**, 1080 (1968)].
¹³V. E. Zubov, Deposited Paper No. 2816 [in Russian], VINITI, Moscow (1979).
¹⁴V. E. Zubov, G. S. Krinchik, and A. D. Kudakov, *Pis'ma Zh. Eksp. Teor. Fiz.* **47**, 134 (1988) [*JETP Lett.* **47**, 161 (1988)].
¹⁵A. Hubert, *Theorie der Domänenwände in geordneten Medien*, Springer Verlag, Berlin (1974).
¹⁶U. Hartmann and H. H. Mende, *Phys. Rev. B* **33**, 4777 (1986); *J. Appl. Phys.* **59**, 4123 (1986).

Translated by A. Tybulewicz